Western Science

# A new perspective on infection forces with demonstration by a DDE infectious disease model

Tianyu Cheng *supervised by* Dr. Xingfu Zou
Department of Mathematics, Western University
tchen454@uwo.ca

## Introduction

During a pandemic or epidemic, due to various control measures, susceptible individuals become less social and more precautions, having less chances of exposing to infectious people.

- **The proportion function** $P$ is the fraction of the susceptible individuals who will actually be possibly exposed to the infectious hosts and hence be possibly infected. The proportion function $P$ depends on *the severity of the epidemic* $L$ and satisfies the following basic assumption:

(H1) $P(L)$ is a monotonic non-increasing function, satisfying $P(0) \leq 1$ and $\lim_{L\to+\infty} P(L) \geq 0$.

- **The severity of epidemics** $L$ evolves with time and can be measured by the infection numbers in previous time interval of fixed length:

$$L(t) = \int_{t-\tau}^{t} w(\xi) I(t-\xi)\, d\xi \tag{1}$$

or by the infection numbers collected at previous fixed number of time points:

$$L(t) = \sum_{j=0}^{n} k_j I(t-\tau_j). \tag{2}$$

- **Practically susceptible population:** is

$$S_p(t) = P(L(t))S(t).$$

- **Revised infection force** is

$$f(t) = \beta I(t) P(L(t)).$$

## Model

A demonstration example:

$$\begin{cases} S'(t) = \Lambda - dS(t) - f(t)S(t) + \alpha R(t), \\ I'(t) = f(t)S(t) - (d+r+\epsilon)I(t), \\ R'(t) = rI(t) - (d+\alpha)R(t). \end{cases} \tag{3}$$

where

$$f(t) = \beta I(t) P(L(t)), \quad L(t) = \sum_{j=0}^{n} k_j I(t-\tau_j), \tag{4}$$

with the proportion function satisfying (H1).

## Parameters

| Parameter | Definition |
|---|---|
| $\Lambda$ | Recruitment rate of the population |
| $d$ | Natural death rate of the population |
| $r$ | Recovery rate of infective individuals |
| $\epsilon$ | Disease-induced death rate |
| $\alpha$ | Rate of removed individuals who lose immunity |
| $\beta$ | Transmission rate |

**Two strategy parameters** :

- $k_j \geq 0$, $j = 0, 1, \cdots, n$ are the discrete weights, satisfying

$$\sum_{j=0}^{n} k_j = 1;$$

- $\tau_0 = 0$ and $0 < \tau_1 < \tau_2 < \cdots < \tau_n$ are the positive numbers that may account for the past $n$ time points at which the infected cases are reported.

## Reduced Model with Particular $P(L(t))$

Consider the following particular severity measurement

$$L(t) = k_0 I(t) + k_1 I(t-\tau),$$

and the exponential decay function for $P(L)$:

$$P(L) = e^{-hL}.$$

The model (3)-(4) is reduced as

$$\begin{cases} S'(t) = \Lambda - dS(t) - \beta I(t) e^{-h(k_0 I(t) + k_1 I(t-\tau))} S(t) + \alpha R(t), \\ I'(t) = \beta I(t) e^{-h(k_0 I(t) + k_1 I(t-\tau))} S(t) - (d+r+\epsilon)I(t), \\ R'(t) = rI(t) - (d+\alpha)R(t). \end{cases} \tag{5}$$

## Theoretical Results

**Basic reproduction number** $R_0$ of the model (3)-(4) :

$$R_0 = \frac{1}{d+r+\epsilon} \cdot [\beta P(0) S_0].$$

- **Disease free equilibrium** $E_0$ for the model (3)-(4)
  - is globally asymptotically stable if $R_0 < 1$;
  - is unstable if $R_0 > 1$, and there occurs a unique endemic equilibrium $E^*$.
- **Endemic equilibrium** $E^*$ **for a particular** $P(L(t))$ has the following four scenarios:
  - $E^*$ is locally asymptotically stable for all $\tau \geq 0$;
  - $E^*$ is locally asymptotically stable for $\tau \in [0, \tau^0)$ and keeps unstable for $\tau > \tau^0$;
  - $E^*$ is locally asymptotically stable for $\tau \in [0, \tau^0)$ and become unstable for $\tau \in [\tau^0, \tau^{0,-})$, then regain its stability for some $\tau > \tau^{0,-}$

under different assumptions on $\tau$ and $k_1$

## Numerical Demonstration

Let $\Lambda = 0.2$, $\beta = 1$, $h = 3$, $d = 0.2$, $r = 0.05$, $\epsilon = 0.1$, $\alpha = 0.06$. Then $\bar{k}_{10} \approx 0.93364$, $\bar{k}_{11} \approx 0.88864$, $\bar{k}_{12} \approx 1.27804$ and $k_c = 0.929195195$.

**Fig1: The first bifurcation branch**

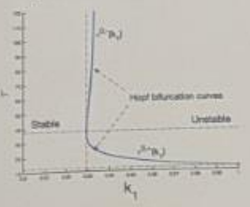

Fig1 shows that

- $0 < k_1 < k_c$, $E^*$ remains stable for all $\tau \geq 0$;
- $k_c < k_1 < \bar{k}_{10}$, *two sequences* of critical values for $\tau$ starting with $\tau^{0,+}$ and $\tau^{0,-}$, respectively. Multiple switches of the stability/instability of $E^*$ as $\tau$ increases;
- $\bar{k}_{10} < k_1 \leq 1$, *only one sequence* of critical values for $\tau$ starting with $\tau^{0,+}$, and $E^*$ loses stability at $\tau = \tau^{0,+}$ remains unstable for all $\tau > \tau^{0,+}$.
- If $\tau < 12.45$, $E^*$ is stable for all $k_1 \in [0, 1]$.

(a). Fix $k_1 = 0.931$; (b) Fix $k_1 = 0.94$.

**Fig2: Real part of roots of the characteristics at $E^*$ in cases (a) and (b)**

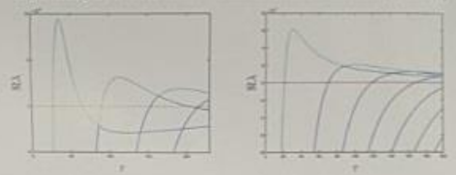

Fig2 shows that *alternating order* of $\tau$ influences switches of stability/instability of $E^*$.

**Fig3: Bifurcation diagram in cases (a) and (b)**

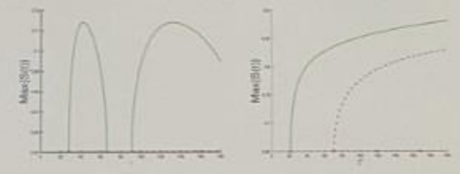

Fig3 shows (a) Stability/instability of $E^*$ switches (b) No switches.

## Discussion

- A new perspective to look at infection forces in modelling infectious disease transmission dynamics;
- A new infection force that depends on both the disease surveillance at current time $t$ and the disease surveillance at a past time $t-\tau$, with each being given a weight ($k_0$ and $k_1$, respectively);
- The *path of Hopf bifurcations* when $\tau$ increases can be different when other model parameters are at different values.
- The long-term effect of control measures changes when the delay in reporting of infection increases;
- Timely reporting is important to management of a disease!

## References

A. Li, Y. Wang, P. Cong, X. Zou, Re-examination of the impact of some non-pharmaceutical interventions and media coverage on the COVID-19 outbreak in Wuhan, *Infect. Dis. Model.*, **6** (2021), 975-987.

P. Song, Y. Xiao, Analysis of an epidemic system with two response delays in media impact function, *Bull. Math. Biol.*, **81** (2019), 1582-1612.

This work has been published in *Mathematical Biosciences and Engineering*, **19(5)** (2022), 4856-4880.

# Predicting Dengue Incidence In Central Argentina Using Google Trends Data

S. Chindal[1], E.L. Estallo[2], Y. Qian[1], M.A. Robert[3]
[1] Department of Statistical Sciences and Operations Research, Virginia Commonwealth University, Richmond, Virginia, USA
[2] Instituto de Investigaciones Biológicas y Tecnológicas, CONICET-Universidad Nacional de Córdoba, Centro de Investigaciones Entomológicas de Córdoba, Córdoba, Argentina
[3] Department of Mathematics, Virginia Tech, Blacksburg, Virginia, USA

## Background

### Dengue

Figure 1: Global spread of dengue virus types mapping the 70-year history[1]

- Mosquito-borne disease in humans
- [illegible] region that has recently been emerging in temperate areas, particularly in the Americas.
- Common symptoms of dengue are headache, fever, exhaustion, muscle and joint pains.
- There is a vaccine for dengue, but it's not widely available.
- Approximately 400 million reported cases & 40,000 deaths from dengue occur each year globally.

Figure 2: Dengue Transmission Pathway

Figure 3: Dengue cases over time in Córdoba, Argentina[2,3]

Figure 4: Córdoba, Argentina[4]

### Córdoba

- City in temperate central Argentina
- No reported dengue cases before 2009
- Several dengue outbreaks have occurred in the last decade, with major outbreaks in 2009, 2013, 2015, 2016, and 2020.

## Questions of Interest

- Can we develop a model that harnesses data from google searches to predict changes in dengue cases?
  - Google Trends (GT) data has been used in the past for prediction of infectious disease spread.
- Is there a relationship between search terms and outbreaks?
- Is there a relationship among search terms?

## Methods

### Data Collection & Analysis

- We obtained time series data for number of search terms from 2016.
- We compared these terms to case counts from the 2016 dengue outbreak in Cordoba.
- We then analyzed relationships between the search terms (predictors) and case data (response) using several methods.

Figure 5: Example of Google Trends Data

Figure 6: Search – case data[2]

### Account for Lag

- We tested lags of up to 6 weeks prior to case counts.
- Lags of 3 weeks were significant for many of the search terms.

### Linear Model & Model Selection

- We constructed a linear model and performed several model selection methods:
  - Forward: Empty model → Add variable one by one
  - Backward: Full model → Remove variable one by one
  - Stepwise: Empty model → Add/Remove variable one by one
- We calculated an adjusted $R^2$, which penalizes for adding insignificant predictors.

### Principal Component Analysis (PCA)

- Principal component (PC):
  - linear combination of all predictors with largest variation in data
- Type of dimension reduction method
- Want to try and preserve as much information as possible with few PCs

### Principal Component Regression (PCR)

- Combination of Linear Regression & PCA
  - Choose and calculate first $n$ PCs
  - Create least squares model using these $n$ PCs & response variable

### Partial Least Squares Regression (PLS)

- Supervised alternative to PCR

## Results

- Below we present the GT search terms from our different methods that have the most significant relationships with dengue cases:

| Method | Terms | Coefficients | Significance |
|---|---|---|---|
| Linear Model | dengue virus | −1.9768 | 0.073 |
| Subset Selection | dengue virus, virus del dengue, dolor de cabeza, fiebre | −1.977, 2.495, −0.940, −0.528 | 0.0147, 0.0665, 0.0411, 0.0390 |

Table 1: Search term results for the model without lag

| Method | Terms | Coefficients | Significance |
|---|---|---|---|
| Linear Model | mosquito, virus del dengue | 0.6970, 3.8167 | 0.028, 0.027 |
| Subset Selection | aedes, mosquito, virus del dengue, fiebre | 0.685, 0.004, 2.799, −0.406 | 0.09858, 0.00012, 0.00852, 0.02411 |

Table 2: Search term results for the model with lag (3 weeks)

| Type | $R^2$ | Adjusted $R^2$ |
|---|---|---|
| Without lag | 0.44036 | 0.0158 |
| With lag | 0.7184 | 0.4801 |

Table 3: Search term results for full model (search terms from linear model in Table 2)

| Type | $R^2$ | Adjusted $R^2$ |
|---|---|---|
| Without lag | 0.26621 | 0.20376 |
| With lag | 0.6675 | 0.6373 |

Table 4: Search term results for reduced model (search terms from subset model in Table 2)

PCR

PLS

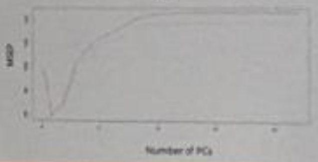

| Model Type | PCA | PCR | PLS |
|---|---|---|---|
| Without lag | PC4 → 74.81%<br>PC7 → 84.85%<br>PC9 → 89.08% | PC4 → 17.27%<br>PC7 → 20.21%<br>PC9 → 26.57% | PC4 → 42.45%<br>PC7 → 43.99%<br>PC9 → 44.03% |
| With lag | PC4 → 74.96%<br>PC7 → 85.39%<br>PC9 → 89.60% | PC4 → 58.88%<br>PC7 → 61.98%<br>PC9 → 62.04% | PC4 → 70.91%<br>PC7 → 71.78%<br>PC9 → 71.83% |

Table 5: PCA, PCR, PLS Results

- In model with lag, about 74.96% of variability in response (dengue cases) is explained by 7 principal components (Table 5).
- PCA performs the best, followed by PLS and PCR (Table 5).

## Conclusions & Future Work

- Significant terms:
  - aedes, mosquito, virus del dengue, fiebre
- It is possible that some search terms are confounding variables because they could be associated with other illnesses like chikungunya or Zika virus.
- We plan to test the efficacy of this model by using it to predict 2020 and 2023 case data.
- We also plan to expand this work by training the model on multiple years of data and testing it against the most recent outbreaks.

## References

1) Messina, J. P., Brady, O. J., Scott, T. W., Zou, C., Pigott, D. M., Duda, K. A., Bhatt, S., Katzelnick, L., Howes, R. E., Battle, K. E., Simmons, C. P., & Hay, S. I. (2014). Global spread of dengue virus types: Mapping the 70 year history. Trends in Microbiology, 22(3), 138-146. [illegible]
2) Ministerio de Salud y Desarrollo Social. Boletines epidemiológicos. [illegible] (2018).
3) Robert, M. A., Tinunin, D. T., Benitez, E. M., Ludueña-Almeida, F. F., Romero, M., Stewart-Ibarra, A. M., & Estallo, E. L. (2019). Arbovirus emergence in the temperate city of Córdoba, Argentina, 2009-2018. Scientific Data, 6(1), 276. [illegible]
4) Romero-Alvarez, D., Parikh, N., Osthus, D., Martinez, K., Generous, N., del Valle, S., & Manore, C. A. (2020). Google Health Trends performance reflecting dengue incidence for the Brazilian states. BMC Infectious Diseases, 20(1), 252. [illegible]

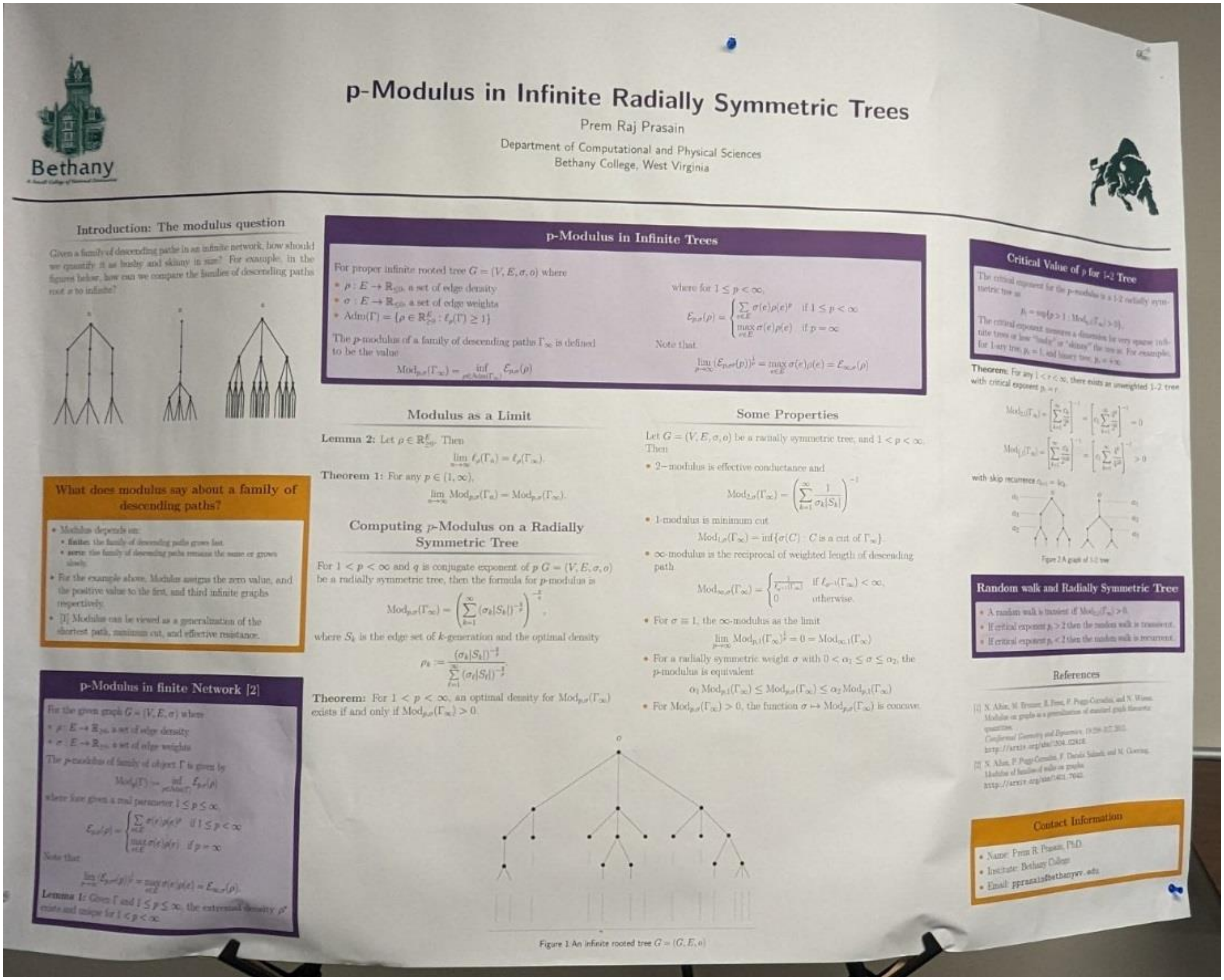

# p-Modulus in Infinite Radially Symmetric Trees

Prem Raj Prasain
Department of Computational and Physical Sciences
Bethany College, West Virginia

## Introduction: The modulus question

Given a family of descending paths in an infinite network, how should we quantify it as bushy and skinny in size? For example, in the figures below, how can we compare the families of descending paths root $o$ to infinite?

## What does modulus say about a family of descending paths?

- Modulus depends on:
  - **finite**: the family of descending paths grows fast.
  - **zero**: the family of descending paths remains the same or grows slowly.
- For the example above, Modulus assigns the zero value, and the positive value to the first, and third infinite graphs respectively.
- [1] Modulus can be viewed as a generalization of the shortest path, minimum cut, and effective resistance.

## p-Modulus in finite Network [2]

For the given graph $G = (V, E, \sigma)$ where

- $\rho : E \to \mathbb{R}_{\geq 0}$, a set of edge density
- $\sigma : E \to \mathbb{R}_{>0}$, a set of edge weights

The $p$-modulus of family of object $\Gamma$ is given by

$$\text{Mod}_p(\Gamma) = \inf_{\rho \in \text{Adm}(\Gamma)} \mathcal{E}_{p,\sigma}(\rho)$$

where for a given a real parameter $1 \leq p \leq \infty$,

$$\mathcal{E}_{p,\sigma}(\rho) = \begin{cases} \sum_{e \in E} \sigma(e)\rho(e)^p & \text{if } 1 \leq p < \infty \\ \max_{e \in E} \sigma(e)\rho(e) & \text{if } p = \infty \end{cases}$$

Note that

$$\lim_{p \to \infty} (\mathcal{E}_{p,\sigma}(\rho))^{\frac{1}{p}} = \max_{e \in E} \sigma(e)\rho(e) = \mathcal{E}_{\infty,\sigma}(\rho).$$

**Lemma 1:** Given $\Gamma$ and $1 \leq p \leq \infty$, the extremal density $\rho^*$ exists and unique for $1 < p < \infty$.

## p-Modulus in Infinite Trees

For proper infinite rooted tree $G = (V, E, \sigma, o)$ where

- $\rho : E \to \mathbb{R}_{\geq 0}$, a set of edge density
- $\sigma : E \to \mathbb{R}_{>0}$, a set of edge weights
- $\text{Adm}(\Gamma) = \{\rho \in \mathbb{R}^E_{\geq 0} : \ell_\rho(\Gamma) \geq 1\}$

The $p$-modulus of a family of descending paths $\Gamma_\infty$ is defined to be the value

$$\text{Mod}_{p,\sigma}(\Gamma_\infty) = \inf_{\rho \in \text{Adm}(\Gamma_\infty)} \mathcal{E}_{p,\sigma}(\rho)$$

where for $1 \leq p < \infty$,

$$\mathcal{E}_{p,\sigma}(\rho) = \begin{cases} \sum_{e \in E} \sigma(e)\rho(e)^p & \text{if } 1 \leq p < \infty \\ \max_{e \in E} \sigma(e)\rho(e) & \text{if } p = \infty \end{cases}$$

Note that

$$\lim_{p \to \infty} (\mathcal{E}_{p,\sigma}(\rho))^{\frac{1}{p}} = \max_{e \in E} \sigma(e)\rho(e) = \mathcal{E}_{\infty,\sigma}(\rho)$$

## Modulus as a Limit

**Lemma 2:** Let $\rho \in \mathbb{R}^E_{\geq 0}$. Then

$$\lim_{n \to \infty} \ell_\rho(\Gamma_n) = \ell_\rho(\Gamma_\infty).$$

**Theorem 1:** For any $p \in (1, \infty)$,

$$\lim_{n \to \infty} \text{Mod}_{p,\sigma}(\Gamma_n) = \text{Mod}_{p,\sigma}(\Gamma_\infty).$$

## Computing $p$-Modulus on a Radially Symmetric Tree

For $1 < p < \infty$ and $q$ is conjugate exponent of $p$ $G = (V, E, \sigma, o)$ be a radially symmetric tree, then the formula for $p$-modulus is

$$\text{Mod}_{p,\sigma}(\Gamma_\infty) = \left( \sum_{k=1}^{\infty} (\sigma_k |S_k|)^{-\frac{q}{p}} \right)^{-\frac{p}{q}},$$

where $S_k$ is the edge set of $k$-generation and the optimal density

$$\rho_k := \frac{(\sigma_k |S_k|)^{-\frac{q}{p}}}{\sum_{\ell=1}^{\infty} (\sigma_\ell |S_\ell|)^{-\frac{q}{p}}}.$$

**Theorem:** For $1 < p < \infty$, an optimal density for $\text{Mod}_{p,\sigma}(\Gamma_\infty)$ exists if and only if $\text{Mod}_{p,\sigma}(\Gamma_\infty) > 0$.

## Some Properties

Let $G = (V, E, \sigma, o)$ be a radially symmetric tree, and $1 < p < \infty$. Then

- 2−modulus is effective conductance and
$$\text{Mod}_{2,\sigma}(\Gamma_\infty) = \left( \sum_{k=1}^{\infty} \frac{1}{\sigma_k |S_k|} \right)^{-1}$$
- 1-modulus is minimum cut
$$\text{Mod}_{1,\sigma}(\Gamma_\infty) = \inf\{\sigma(C) : C \text{ is a cut of } \Gamma_\infty\}.$$
- $\infty$-modulus is the reciprocal of weighted length of descending path
$$\text{Mod}_{\infty,\sigma}(\Gamma_\infty) = \begin{cases} \frac{1}{\ell_{\sigma^{-1}}(\Gamma_\infty)} & \text{if } \ell_{\sigma^{-1}}(\Gamma_\infty) < \infty, \\ 0 & \text{otherwise.} \end{cases}$$
- For $\sigma \equiv 1$, the $\infty$-modulus as the limit
$$\lim_{p \to \infty} \text{Mod}_{p,1}(\Gamma_\infty)^{\frac{1}{p}} = 0 = \text{Mod}_{\infty,1}(\Gamma_\infty)$$
- For a radially symmetric weight $\sigma$ with $0 < \alpha_1 \leq \sigma \leq \alpha_2$, the $p$-modulus is equivalent
$$\alpha_1 \text{Mod}_{p,1}(\Gamma_\infty) \leq \text{Mod}_{p,\sigma}(\Gamma_\infty) \leq \alpha_2 \text{Mod}_{p,1}(\Gamma_\infty)$$
- For $\text{Mod}_{p,\sigma}(\Gamma_\infty) > 0$, the function $\sigma \mapsto \text{Mod}_{p,\sigma}(\Gamma_\infty)$ is concave.

Figure 1:An infinite rooted tree $G = (G, E, o)$

## Critical Value of $p$ for 1-2 Tree

The critical exponent for the p-modulus in a 1-2 radially symmetric tree as

$$p_c = \sup\{p > 1 : \text{Mod}_{p,1}(\Gamma_\infty) > 0\}.$$

The critical exponent measures a dimension for very sparse infinite trees or how "bushy" or "skinny" the tree is. For example, for 1-ary tree, $p_c = 1$, and binary tree, $p_c = +\infty$.

**Theorem:** For any $1 < r < \infty$, there exists an unweighted 1-2 tree with critical exponent $p_c = r$.

$$\text{Mod}_{2,1}(\Gamma_\infty) = \left[ \sum_{k=1}^{\infty} \frac{a_k}{2^k} \right]^{-1} = \left[ c \sum_{k=1}^{\infty} \frac{k^p}{2^k} \right]^{-1} = 0$$

$$\text{Mod}_{p,1}(\Gamma_\infty) = \left[ \sum_{k=1}^{\infty} \frac{a_k}{2^{k/p}} \right]^{-1} = \left[ c \sum_{k=1}^{\infty} \frac{k^p}{2^{k/p}} \right]^{-1} > 0$$

with skip recurrence $a_{k+1} = ka_k$

Figure 2:A graph of 1-2 tree

## Random walk and Radially Symmetric Tree

- A random walk is transient if $\text{Mod}_{2,1}(\Gamma_\infty) > 0$.
- If critical exponent $p_c > 2$ then the random walk is transient.
- If critical exponent $p_c < 2$ then the random walk is recurrent.

## References

[1] N. Albin, M. Brunner, R. Perez, P. Poggi-Corradini, and N. Wiens. Modulus on graphs as a generalization of standard graph theoretic quantities. *Conformal Geometry and Dynamics*, 19:298–317, 2015. http://arxiv.org/abs/1504.02418

[2] N. Albin, P. Poggi-Corradini, F. Darabi Sahneh, and M. Goering. Modulus of families of walks on graphs. http://arxiv.org/abs/1401.7640

## Contact Information

- Name: Prem R. Prasain, PhD
- Institute: Bethany College
- Email: `pprasain@bethanywv.edu`

# Elucidating Resistance Mechanism to Last Resort Antibiotic Colistin in Critical Priority Pathogen

Jenna Kuhn, Y. Peter Di
Department of Environmental and Occupational Health, University of Pittsburgh School of Public Health
Pitt PublicHealth

## Introduction

**Antimicrobial Resistance Threat:**

- Urgent global health threat contributing to almost 1.3 million deaths worldwide
- 2.8 antimicrobial resistant deaths each year killing over 35,000

***Klebsiella Pneumoniae* (*KP*):**

- Pathogen of Urgent concern for antimicrobial development (CDC)
- Recent convergence of multidrug resistance and hypervirulence
- Global prevalence of nosocomial multidrug-resistant *KP* is estimated to be 32.8%[1]

**Colistin (Polymyxin E):**

- Last resort antibiotic for multidrug-resistant gram-negative bacterial infections
- Resistance continues to be identified

## Study Goals

1. Study the timing and association of colistin resistance (COL-R) mutations in genes having different functional roles through experimental evolution
2. Study the potential synergistic or additive effects of identified critical COL-R mutations

## Methods

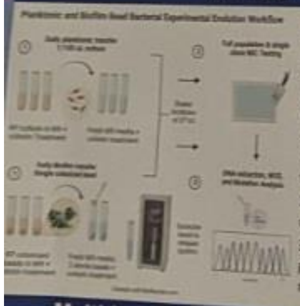

**FIGURE 1: Study Workflow.** 1) Serial transfer of 1:100 bacteria culture or single colonized biofilm bead into M9 media + colistin. Colistin selection began at ½ MIC level and was doubled every three days. 2) Minimum inhibitory concentration (MIC) testing 3) DNA extraction, whole genome sequencing, and mutation prediction analysis

## Multidrug Resistant Clinical Isolates

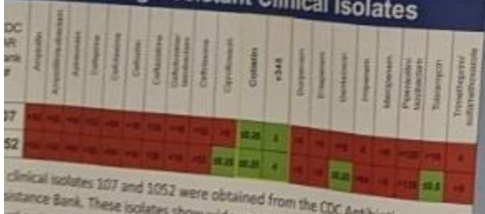

Clinical isolates 107 and 1052 were obtained from the CDC Antibiotic Resistance Bank. These isolates show widespread drug resistance. Colistin and novel antimicrobial peptide v345 inhibit the growth of these "superbugs".

## Colistin Selection Pressure Induces Significant AR

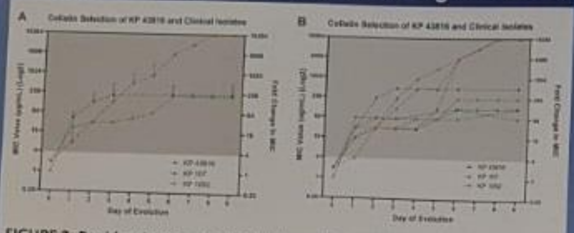

**FIGURE 2: Rapid resistance acquired during colistin-selection of *KP* strains.** *KP* ATCC 43816 and clinical isolates 107 and 1052 sampled from patients with MDR bacterial infections were subject to a 9-day colistin selection. **A)** MIC averaged among 3 replicate populations and **B)** individual population MIC results.

## Temporal Regulation of COL-R in Hypervirulent *KP*

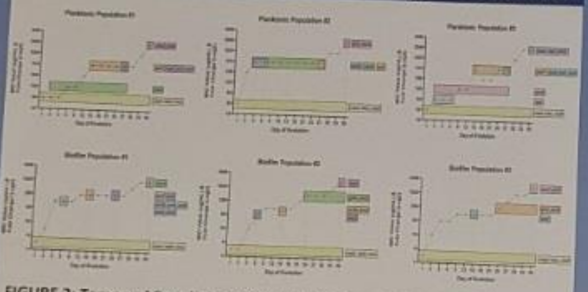

**FIGURE 3: Temporal Regulation of COL-R Mutations in *KP*.** Timelines of mutations generated on known and theorized COL-R genes throughout a 36-day *in-vitro* experimental evolution. The duration of time by which the COL-R mutations (having mutation frequencies greater than 10%) exist within each individual colistin-treated *KP* population is compared against colistin MIC.

## COL-R Pathways in Hv-*KP*

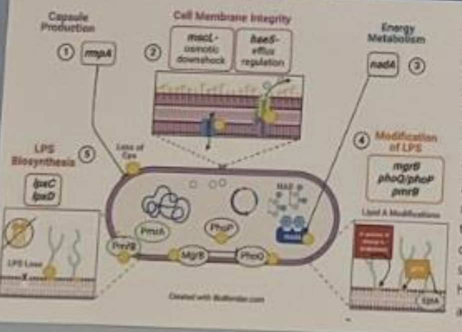

**FIGURE 4: Summary of COL-R Resistance Pathways in Hypervirulent *KP*.** The functional role of COL-R genes and the timing of associated mutations throughout a 36-day colistin-selection in hypervirulent *KP* are noted.

## Timing of COL-R Mutations by Gene Function

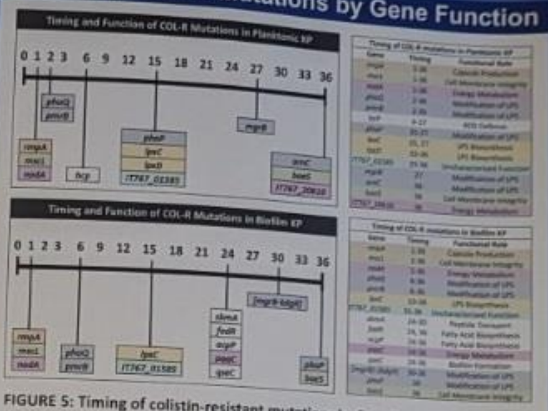

**FIGURE 5: Timing of colistin-resistant mutations by functional role for independent *KP* lifestyles.** Mutations are listed in relation to the first appeared time during evolution and color coded by functional role to compare COL-R resistance patterns in planktonic and biofilm lifestyles. The timing in which of shared mutations are generated and their corresponding functions can be compared between planktonic and biofilm-evolved *KP*.

## Conclusions and Future Directions

- **A mutation in *rmpA* may be a critical factor for initiating resistance through loss of capsule production**
- **Additional mutations affecting different functional pathways could occur sequentially or simultaneously**
- **The timing of resistance mutations may largely impact COL-R progression**
- **Mutation function and impact on virulence are being studied using CRISPR-based approaches**
- **Colistin-resistant *KP* 43816 remains susceptible to dual antibiotic Ceftazidime/Avibactam (CAZ-AVI) (Figure 6).**

**Figure 6. Colistin resistant, Hv*KP* does not generate cross-resistance to CAZ-AVI.** Following 36 days of experimental evolutions of *KP* ATCC 43816 under colistin selection, CAZ-AVI inhibits growth well below the clinical breakpoint of 16 μg/mL (shaded grey).

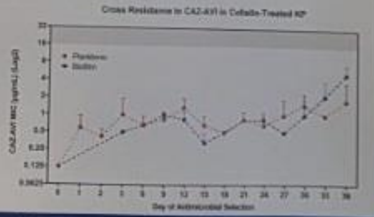

## Acknowledgements & References

This research was funded by the National Institutes of Health (R01 AI133351)

1.) Mohd Asri NA, Ahmad S, Mohamud R, Mohd Hanafi N, Mohd Zaidi NF, Irekeola AA, Shueb RH, Yee LC, Mohd Noor N, Mustafa FH, Yean CY, Yusof NY. Global Prevalence of Nosocomial Multidrug-Resistant Klebsiella pneumoniae: A Systematic Review and Meta-Analysis. Antibiotics (Basel). 2021 Dec 8;10(12):1508. doi: 10.3390/antibiotics10121508. PMID: 34943720; PMCID: PMC8698758.
2) Kuhn JM, Di YP. Determination of Mutational Timing of Colistin-Resistance Genes through Klebsiella pneumoniae Evolution. Pharmaceutics. 2023 Jan 12;15(1):270. doi: 10.3390/pharmaceutics15010270. PMID: 36678901; PMCID: PMC9862994.

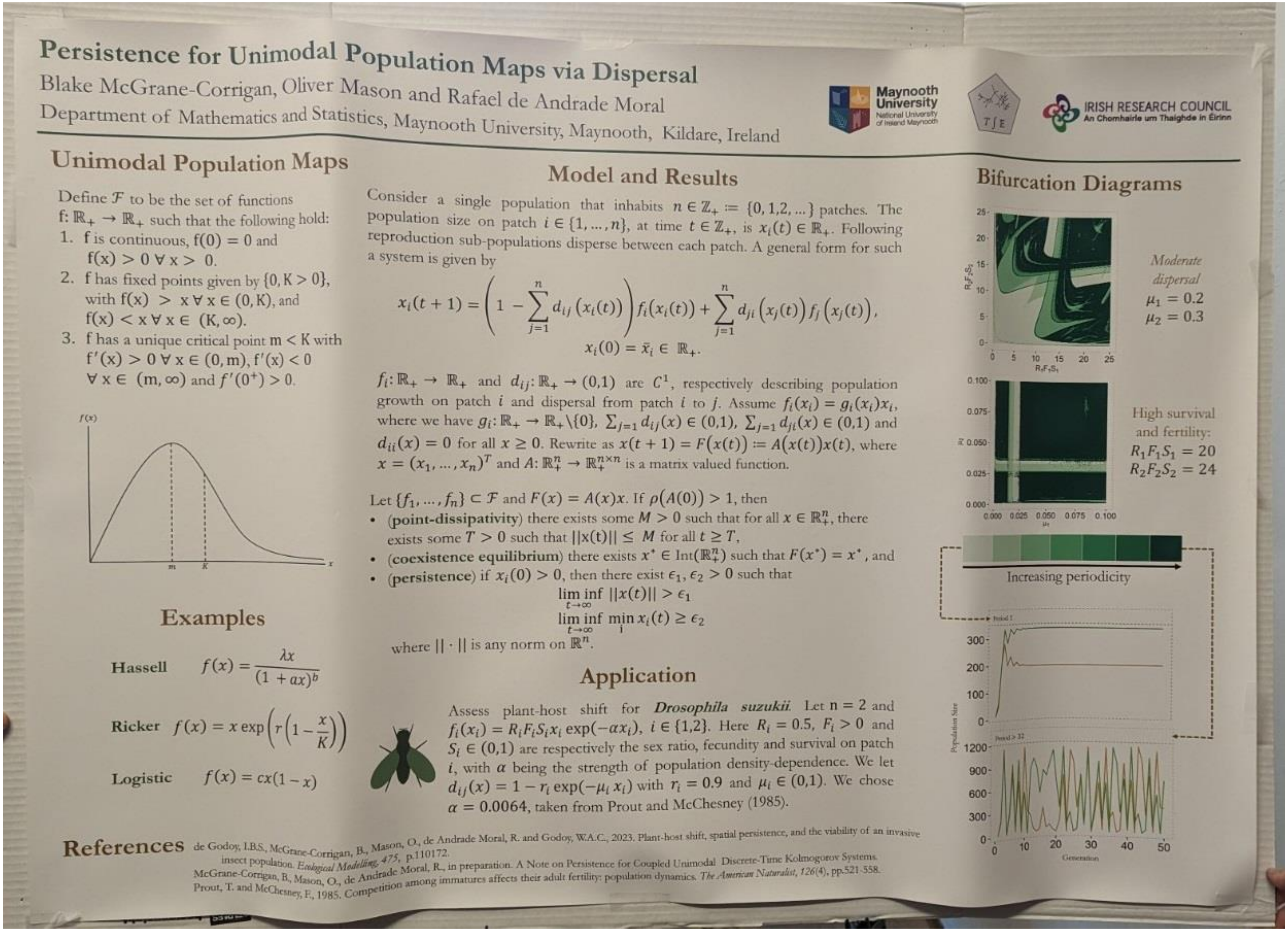

# Persistence for Unimodal Population Maps via Dispersal

Blake McGrane-Corrigan, Oliver Mason and Rafael de Andrade Moral
Department of Mathematics and Statistics, Maynooth University, Maynooth, Kildare, Ireland

Maynooth University
National University of Ireland Maynooth

IRISH RESEARCH COUNCIL
An Chomhairle um Thaighde in Éirinn

## Unimodal Population Maps

Define $\mathcal{F}$ to be the set of functions $f: \mathbb{R}_+ \to \mathbb{R}_+$ such that the following hold:

1. f is continuous, $f(0) = 0$ and $f(x) > 0 \; \forall x > 0$.
2. f has fixed points given by $\{0, K > 0\}$, with $f(x) > x \; \forall x \in (0, K)$, and $f(x) < x \; \forall x \in (K, \infty)$.
3. f has a unique critical point $m < K$ with $f'(x) > 0 \; \forall x \in (0, m)$, $f'(x) < 0 \; \forall x \in (m, \infty)$ and $f'(0^+) > 0$.

## Examples

**Hassell** $f(x) = \dfrac{\lambda x}{(1 + ax)^b}$

**Ricker** $f(x) = x \exp\left(r\left(1 - \dfrac{x}{K}\right)\right)$

**Logistic** $f(x) = cx(1 - x)$

## Model and Results

Consider a single population that inhabits $n \in \mathbb{Z}_+ := \{0, 1, 2, \dots\}$ patches. The population size on patch $i \in \{1, \dots, n\}$, at time $t \in \mathbb{Z}_+$, is $x_i(t) \in \mathbb{R}_+$. Following reproduction sub-populations disperse between each patch. A general form for such a system is given by

$$x_i(t+1) = \left(1 - \sum_{j=1}^{n} d_{ij}\left(x_i(t)\right)\right) f_i(x_i(t)) + \sum_{j=1}^{n} d_{ji}\left(x_j(t)\right) f_j\left(x_j(t)\right),$$
$$x_i(0) = \bar{x}_i \in \mathbb{R}_+.$$

$f_i: \mathbb{R}_+ \to \mathbb{R}_+$ and $d_{ij}: \mathbb{R}_+ \to (0,1)$ are $C^1$, respectively describing population growth on patch $i$ and dispersal from patch $i$ to $j$. Assume $f_i(x_i) = g_i(x_i)x_i$, where we have $g_i: \mathbb{R}_+ \to \mathbb{R}_+ \setminus \{0\}$, $\sum_{j=1} d_{ij}(x) \in (0,1)$, $\sum_{j=1} d_{ji}(x) \in (0,1)$ and $d_{ii}(x) = 0$ for all $x \geq 0$. Rewrite as $x(t+1) = F(x(t)) := A(x(t))x(t)$, where $x = (x_1, \dots, x_n)^T$ and $A: \mathbb{R}_+^n \to \mathbb{R}_+^{n \times n}$ is a matrix valued function.

Let $\{f_1, \dots, f_n\} \subset \mathcal{F}$ and $F(x) = A(x)x$. If $\rho(A(0)) > 1$, then

- (**point-dissipativity**) there exists some $M > 0$ such that for all $x \in \mathbb{R}_+^n$, there exists some $T > 0$ such that $||x(t)|| \leq M$ for all $t \geq T$,
- (**coexistence equilibrium**) there exists $x^* \in \mathrm{Int}(\mathbb{R}_+^n)$ such that $F(x^*) = x^*$, and
- (**persistence**) if $x_i(0) > 0$, then there exist $\epsilon_1, \epsilon_2 > 0$ such that

$$\liminf_{t \to \infty} ||x(t)|| > \epsilon_1$$
$$\liminf_{t \to \infty} \min_i x_i(t) \geq \epsilon_2$$

where $|| \cdot ||$ is any norm on $\mathbb{R}^n$.

## Application

Assess plant-host shift for ***Drosophila suzukii***. Let $n = 2$ and $f_i(x_i) = R_i F_i S_i x_i \exp(-\alpha x_i)$, $i \in \{1,2\}$. Here $R_i = 0.5$, $F_i > 0$ and $S_i \in (0,1)$ are respectively the sex ratio, fecundity and survival on patch $i$, with $\alpha$ being the strength of population density-dependence. We let $d_{ij}(x) = 1 - r_i \exp(-\mu_i x_i)$ with $r_i = 0.9$ and $\mu_i \in (0,1)$. We chose $\alpha = 0.0064$, taken from Prout and McChesney (1985).

## Bifurcation Diagrams

*Moderate dispersal*
$\mu_1 = 0.2$
$\mu_2 = 0.3$

High survival and fertility:
$R_1F_1S_1 = 20$
$R_2F_2S_2 = 24$

Increasing periodicity

## References

de Godoy, I.B.S., McGrane-Corrigan, B., Mason, O., de Andrade Moral, R. and Godoy, W.A.C., 2023. Plant-host shift, spatial persistence, and the viability of an invasive insect population. *Ecological Modelling*, *475*, p.110172.
McGrane-Corrigan, B., Mason, O., de Andrade Moral, R., in preparation. A Note on Persistence for Coupled Unimodal Discrete-Time Kolmogorov Systems.
Prout, T. and McChesney, F., 1985. Competition among immatures affects their adult fertility: population dynamics. *The American Naturalist*, *126*(4), pp.521-558.

# HOW DOES TEMPORAL VARIATION IN IMMIGRATION AFFECT POPULATION DYNAMICS?

**Sikander B. Khare and Robert D. Holt**
Department of Biology, University of Florida, Gainesville, FL 32611

## INTRODUCTION

- Empirically observed dispersal rates can be highly variable but have not been fully explored in theoretical models
- Variation in dispersal rates can be caused by exogenous and endogenous drivers[1]

| Exogenous drivers | Endogenous drivers |
|---|---|
| • passively dispersed organisms<br>• temperature dependent dispersal rates[2]<br>• seasonal changes in landscape connectivity[3] | • fluctuations in population density[4]<br>• sex ratio[5]<br>• phenotypic composition |

- We use peripheral populations as a *limiting case*
- We examine the effects of constant vs. varying immigration

**Figure 1:** Schematic diagram of a peripheral population receiving immigration from a source a population

## MODELS

1. Ricker model with immigration

$$N_{t+1} = N_t \exp\left[r\left(1 - \frac{N_t}{K}\right)\right] + I_t$$

2. Rosenzweig-MacArthur model with immigration

$$\frac{dN}{dt} = N\left[r - dN - \frac{aP}{1 + ahN}\right]$$

$$\frac{dP}{dt} = P\left(\frac{abN}{1 + ahN} - m\right) + I(t)$$

## MODEL 1 RESULTS: CYCLICAL IMMIGRATION

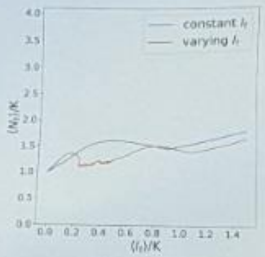

**Figure 2** (*above*): Average density for constant and temporally varying $I_t$. Constant $I_t = I$. Time-varying $I_t$ is a 2-cycle between $I_t = 0$ and $I_{t+1} = 2I$

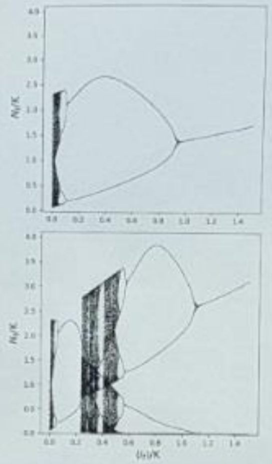

**Figure 3** (*right*): (*Top*) Bifurcation plot for constant $I_t$. (*Bottom*) Bifurcation plot for and temporally varying $I_t$.

## MODEL 2 RESULTS: PULSED IMMIGRATION

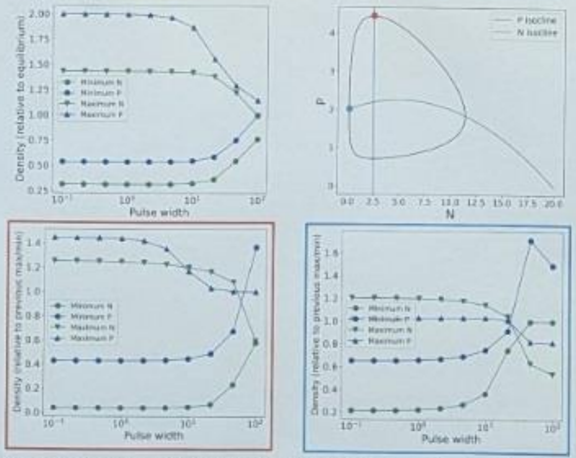

**Figure 4:** Transient response to pulsed immigration. Width of square pulse is varied, while pulse area (total immigration) is kept the same. (*Top left*) Response for a system with stable equilibrium dynamics. (*Top right*) Isocline diagram with limit cycle. Colored dots correspond to where the system has been perturbed for the results in the bottom panels. (*Bottom*) Panel border colors correspond to dots in top left panel

## MODEL 2 RESULTS: CYCLICAL IMMIGRATION

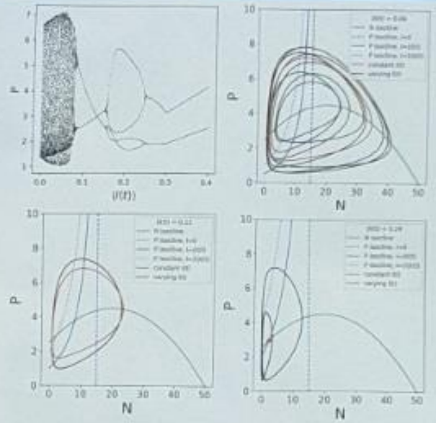

**Figure 5:** Comparing constant vs. sinusoidal immigration with same average immigration rate. (Top left) Bifurcation diagram produced by stroboscopic sampling of timeseries. (Top right) Cyclical dynamics become chaotic. (Bottom left) Limit cycle changes trajectory. (Bottom left) Stable dynamics become cyclical with period-doubling effect

## CONCLUSIONS

- Immigration stabilizes population after a certain point
- Increase in immigration does not necessarily lead to higher density
- Transient effect of pulsed immigration depends on where in the cycle the perturbation occurs
- Cyclical immigration can qualitatively change the dynamics of the system
- Future directions:
  - Predator-prey with Allee effects in prey species
  - Apparent competition module

## REFERENCES

1. Peniston, J. H., et al. 2023 (under revision). Ecological and evolutionary consequences of temporal variation in dispersal. Ecography
2. Gibert, J. P. et al. 2016. Crossing regimes of temperature dependence in animal movement. - Global Change Biology 22: 1722–1736.
3. Uroy, L. et al. 2021. How to assess the temporal dynamics of landscape connectivity in ever-changing landscapes: a literature review. - Landscape Ecol 36: 2487–2504.
4. Matthysen, E. 2005. Density-dependent dispersal in birds and mammals. - Ecography 28: 403–416
5. Sandell, M. et al. 1990. Natal dispersal in relation to population density and sex ratio in the field vole, Microtus agrestis. - Oecologia 83: 145–149.

# REDDUST

## Random Effect Delay Difference model with User Specified Timestep

Montana Wickens, Brisbane, Australia

## What?

REDDUST is a fishery population model developed for data-limited species to aid the formal process of stock assessments. REDDUST allows for monthly, bimonthly, trimonthly, quadmonthly, semi-annual and annual biomass dynamics with seasonal variation in recruitment, spawning and catchability and extends current methods by treating annual recruitment variations as random effects.

## Where?

REDDUST was developed for data-limited fisheries in Queensland, Australia such as the East Coast Otter Trawl Fishery comprised mostly of prawns, scallops and bugs.

## Basic Stock Assessment:

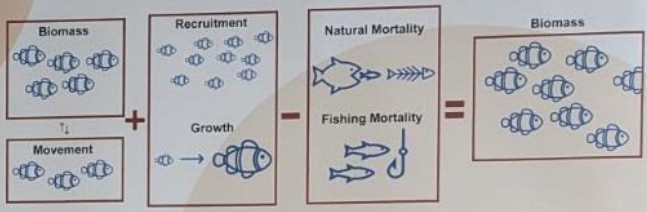

Biomass

Movement

\+

Recruitment

Growth

−

Natural Mortality

Fishing Mortality

=

Biomass

## Why?

The delay difference model is ideal for fisheries that have the data to support mild complexity - described as being between surplus production models and full age-structured models - which is often the case for crustaceans and shellfish. The delay difference model can also be extended to capture fine-scale growth, recruitment and mortality by reducing the time step between delays. The adaptive time step makes the model useful for shorter-lived species that have complex intra-annual biomass dynamics.

## LANGUAGE

REDDUST is written using TMB (Template Model Builder) - an R package for fitting statistical latent variable models to data. TMB requires the model is formulated in C++. Some benefits of TMB are:

- TMB can calculate first and second order derivatives of the likelihood function by **automatic-differentiation**, or any objective function written in C++.
- The objective function (and its derivatives) can be called from R. Hence, parameter estimation via nlminb() is easy.
- The user can specify that the **Laplace approximation** should be applied to any subset of the function arguments - yielding **marginal likelihood** in latent variable model.
- **Standard deviations** of any parameter, or derived parameter, obtained by the 'delta method'.
- TMBstan for simple MCMC simulation.
- Hessian calculated for optimisation speed/accuracy, convergence testing, parameter correlation.

## The Model

The population dynamics are governed by the delay difference model, equation 5.15 of Quinn & Deriso Quinn II et al. 2000.

$$B_t = (1+\rho)s_{t-1}B_{t-1} - \rho s_{t-1}s_{t-2}B_{t-2} - \rho s_{t-1}w_{r-1}R_{t-1} + w_r R_t$$
$$N_t = N_{t-1}s_{t-1} + R_t$$

The recruitment is calculated from the spawning biomass from the previous year using the Beverton-Holt equation and distributed according to the recruitment pattern $\phi$.

$$R_t = \phi_{\mathrm{mod}(t,dt)} \frac{\sum_{t'} SB_{t'}}{\alpha + \beta \sum_{t'} SB_{t'}}$$

Deviations from the annual recruitment $R_t$ are treated as fixed effects in DDUST and random effects in REDDUST by integrating the recruitment parameters out of the likelihood. In REDDUST, the relationship between the annual recruitment $R_t$ and the deviated recruitment $R_t^*$ is as follows,

$$R_t^* = R_t e^{\eta_t - \sigma_R^2/2}, \qquad e^{\eta_t} \sim Lognormal(0, \sigma_R^2)$$

The recruitment pattern indicates how the recruits are distributed among the year and is governed by two parameters $\kappa$ and $\mu$ which can be fixed or estimated by the model. The monthly recruitment pattern is assumed to follow an exponential cosine function.

$$\phi_t = \frac{\exp\left(\kappa \cos\frac{2\pi(t-\mu)}{12}\right)}{\sum_{t'=1}^{12} \exp\left(\kappa \cos\frac{2\pi(t'-\mu)}{12}\right)}, \qquad t \in \{1, \dots, 12\}$$

The likelihood has four main components: abundance indices log-likelihood, recruitment deviation log-likelihood, penalties and priors.

$$LL_I = \frac{\log(\sigma_I)}{2} + \sum_t \frac{\log(\hat{I}_t - I_t)^2}{2\sigma_I^2}$$
$$LL_R = \frac{\log(\sigma_R)}{2} + \sum_t \frac{\log(R_t^* - R_t)^2}{2\sigma_R^2}$$

The catch penalty prevents the catch from exceeding the exploitable biomass. An optional recruitment penalty prevents the model from estimating a stupidly high value of initial recruitment by penalising the model if the catch is less than 5% of the recruits. Priors are used to assist in convergence of the optimising algorithm of to preference known biological estimates.

## How do we incorporate environmental variables?

In developing REDDUST, it would benefit the user to optionally include environmental variables in a flexible way. Many economically important species in Australia experience environment-driven population changes. For example, it is theorised that barramundi and king threadfin have large recruitment events after floods and snapper may chase the cooler waters and experience a southern range shift.

Without compromising the parsimony of the delay-difference model, what is the best way to incorporate environmental variables in a statistical sound and meaningful way?

**References**

Courtney, A. J., M. F. O'Neill, M. Braccini, G. M. Leigh, M. Kienzle, S. Pascoe, A. J. Prosser, Y.-G. Wang, L. Lloyd-Jones, A. B. Campbell, M. Ives, S. S. Montgomery, and J. Gorring (Apr. 2014). Biological and economic management strategy evaluations of the eastern king prawn fishery.

Dichmont, C., A. Punt, A. Deng, Q. Dell, and W. Venables (2003). "Application of a weekly delay-difference model to commercial catch and effort data for tiger prawns in Australia's Northern Prawn Fishery". In: Fisheries Research 65.1. Life Histories, Assessment and Management of Crustacean Fisheries, pp. 335–350.

Dichmont, C. M., R. A. Deng, N. Dowling, and A. E. Punt (2021). "Collating stock assessment packages to improve stock assessments". In: Fisheries Research 236, p. 105844.

Haddon, M. (2001). Modelling and quantitative methods in fisheries. Vol. 10, pp. 276–284.

Hilborn, R. and C. J. Walters (1992). "Delay Difference Models". In: Quantitative Fisheries Stock Assessment: Choice, Dynamics and Uncertainty. Boston, MA: Springer US, pp. 330–348.

Maunder, M. N. and R. B. Deriso (2003). "Estimation of recruitment in catch-at-age models". In: Canadian Journal of Fisheries and Aquatic Sciences 60.10. Cited by: 64, pp. 1204–1216.

Methot, R. and I. Taylor (Oct. 2011). "Adjusting for bias due to variability of estimated recruitments in fishery assessment models". In: Canadian Journal of Fisheries and Aquatic Sciences 68, pp. 1744–1760.

Punt, A. E. (2023). "Those who fail to learn from history are condemned to repeat it: A perspective on current stock assessment good practices and the consequences of not following them". In: Fisheries Research 261, p. 106642.

Quinn II, T. J. and R. B. Deriso (Sept. 2000). Quantitative Fish Dynamics. Vol. 75. 3, pp. 208–238. von Bertalanffy, L. (1938). A quantitative theory of organic growth. Vol. 10. 2, pp. 181–213.